High-order harmonic generation of CO_2 with different vibrational modes in an intense laser field*

Hui Du(杜慧), Hong-Dan Zhang(张宏丹), Jun Zhang(张军), Hai-Feng Liu(刘海凤), Xue-Fei Pan(潘雪飞), Jing Guo(郭静), Xue-Shen Liu(刘学深)†

Institute of Atomic and Molecular Physics, Jilin University, Changchun 130012, *China*

(Received 23 June 2016; revised manuscript received 18 July 2016; published online 30 September 2016)

We apply the strong-field Lewenstein model to demonstrate the high-order harmonic generation of CO_2 with three vibrational modes (balance vibration, bending vibration, and stretching vibration) driven by an intense laser field. The results show that the intensity of harmonic spectra is sensitive to molecular vibrational modes, and the high harmonic efficiency with stretching vibrational mode is the strongest. The underlying physical mechanism of the harmonic emission can be well explained by the corresponding ionization yield and the time–frequency analysis. Finally, we demonstrate the attosecond pulse generation with different vibrational modes and an isolated attosecond pulse with a duration of about 112 as is generated.

Keywords: high-order harmonic generation, balance vibration, bending vibration, stretching vibration, isolated attosecond pulse

PACS: 32.80.Rm, 42.65.Ky, 42.65.Re **DOI:** 10.1088/1674-1056/25/11/113201

1. Introduction

High-order harmonic generation (HHG) has been long investigated for its potential applications in modern physics.[1–6] The basic understanding of the high harmonic emission can be provided by the three-step model.[7–9] Electrons are ionized by tunneling to the continuum state; then the freed electrons move with oscillation of the electronic field and after the electric field changes the direction, the electrons may be captured by the parent ion again, radiating high energy harmonic photons. The harmonic spectrum is sensitive to the structure of molecules and induced dynamics, which makes HHG a promising tool to access ultrafast molecular imaging, observation of electron dynamics and molecular structures.[10–12]

With the development of ultrafast laser pulse technology, HHG from molecules has been investigated both theoretically and experimentally.[13–16] Studies on two-center system such as H_2^+ and H_2 showed that the nuclear motion can weaken the efficiency of molecular HHG.[17,18] Spectral minimum induced by two-center interference in HHG from diatomic molecules such as N_2, O_2, CO also contains the information of molecular orbital and structures.[19,20] For the three-center system, a rich set of physical phenomena has attracted a lot of attention. The orbital density imaging of H_2O has been realized by the calculation of the orientation-dependent ionization yield.[21] The HHG of the equilateral H_3^+ was investigated in numerical solutions of the time-dependent Schrödinger equation (TDSE), and the results indicated that the harmonic emission largely depends on the laser–molecule orientation and internuclear distance.[22] Qin *et al.*[23] demonstrated that the interference of the HHG spectra from CO_2 at different alignment angles can modulate the spectra efficiently. It has also been shown that the HHG from CO_2 is very sensitive to multiple molecular orbitals that the effect of the highest occupied molecular orbital (HOMO) and HOMO-2 is important at small alignment angles and only HOMO becomes dominant at large alignment angles.[24,25] Chen *et al.*[26] revealed that the ionization process can remarkably influence the intersections of the HHG spectra from O_2 and CO_2 molecules at different orientation angles. Moreover, the ultrafast molecular imaging of CO_2 has become possible by electron diffraction[27] or extracting the photoelectron momentum spectra of CO_2 probed with circularly polarized laser pulse.[28] Some other polyatomic molecules have also begun to generate further interest. The harmonic yield on different angles between the molecular axis and the laser polarization has proved to contain the fingerprint of the highest occupied molecular orbitals in acetylene and allene, which agrees with the numerical results.[29] Le *et al.*[30] proposed an efficient method of the quantitative rescattering theory (QRS) for calculation of HHG from CCl_4 molecule, which well reproduces the minimum in HHG spectra observed in available experiments. It has also been reported that the HHG intensity can be enhanced with armchair grapheme since the initial electron density distribution along the x axis is much larger than that along the y axis.[31] Very recently, harmonic emission in benzene with linearly and circularly polarized laser pulses has illustrated that the ionic motion has a large effect on the harmonic response.[32]

Here we demonstrate the HHG of CO_2 with different vi-

*Project supported by the National Natural Science Foundation of China (Grant Nos. 61575077, 11271158, and 11574117).

†Corresponding author. E-mail: liuxs@jlu.edu.cn

© 2016 Chinese Physical Society and IOP Publishing Ltd

brational modes (balance vibration, bending vibration, stretching vibration) driven by an intense laser field. The results show that the high harmonic efficiency of CO_2 with stretching vibrational mode is the strongest. The underlying physical mechanism of the HHG can be well explained by the corresponding ionization yield and the time–frequency analysis. When the CO_2 molecule with stretching vibrational mode is exposed in the intense laser field with $\tau_d = 3$ fs, a strong and single attosecond (asec) pulse can be generated.

2. Method

The calculations performed in this paper are based on the strong-field Lewenstein model, which has been widely used to investigate the process of harmonic emission.[7,33,34] The transition amplitude has the form of

$$\begin{aligned} x(t) = \mathrm{i}\int_0^\infty \mathrm{d}\tau \left(\frac{\pi}{\varepsilon + \mathrm{i}\frac{\tau}{2}}\right)^{3/2} & d_z^*[p_{\mathrm{st}}(t,\tau) - A(t)] \\ & \times d_z[p_{\mathrm{st}}(t,\tau) - A(t-\tau)]E(t-\tau) \\ & \times \exp[-\mathrm{i}S(p_{\mathrm{st}},t,\tau)] + \mathrm{c.c.}, \end{aligned} \tag{1}$$

where $E(t)$ is the driving field and $A(t)$ is its associated vector potential. ε is the positive regularization constant, τ is the interval of the ionized electron between ionization and recombination. $S(p_{\mathrm{st}},t,\tau)$ represents that the quasi-classical action at the stationary points can be calculated by

$$S(p_{\mathrm{st}},t,\tau) = \tau I_{\mathrm{p}} - \frac{1}{2}p_{\mathrm{st}}^2(t,\tau) + \frac{1}{2}\int_{t'}^{t} A^2(t'')\,\mathrm{d}t'', \tag{2}$$

where $p_{\mathrm{st}}(t,\tau)$ is the stationary momentum, which can be written as

$$p_{\mathrm{st}}(t,\tau) = \frac{1}{\tau}\int_{t'}^{t} A(t')\,\mathrm{d}t''. \tag{3}$$

The harmonic spectrum intensity is proportional to the Fourier transformation of the time-dependent dipole acceleration

$$P_a(\omega) \sim \left|\frac{1}{T-t_0}\int_{t_0}^{T} x(t)\,\mathrm{e}^{-\mathrm{i}\omega t}\,\mathrm{d}t\right|^2. \tag{4}$$

By superposing several orders of the harmonic spectrum (here q is the harmonic order) we can obtain an attosecond pulse as follows:

$$I(t) = \left|\Sigma a_q\,\mathrm{e}^{\mathrm{i}\omega q t}\right|^2, \tag{5}$$

$$a_q = \int x(t)\,\mathrm{e}^{-\mathrm{i}q\omega t}\,\mathrm{d}t. \tag{6}$$

3. Numerical results

The highest occupied molecular orbital (HOMO) of CO_2 molecule is constructed by the GAMESS-UK package,[35] which is used as the initial input. In the gas phase, the CO_2 molecule has three internal vibrations: the balance vibrational mode (the atoms symmetrically stretch along the molecular axis), bending vibrational mode, and stretching vibrational mode (the atoms asymmetrically stretch along the molecular axis). The three different vibrational modes are taken into account and the corresponding electron density of coordinate–space orbital $|\varphi(r)|^2$ is shown in Fig. 1. The density distribution is very sensitive to the molecular vibrational modes and shows different characteristics depending on different vibrational modes. We can see from Figs. 1(a)–1(c), the electron density distribution of the balance vibrational mode has a "mirror symmetry" structure, which is broken in bending and stretching vibrational modes and gradually converges.

We apply the strong-field Lewenstein model to demonstrate the HHG of CO_2 in a linearly polarized laser field, which has the form as $E(t) = E_0 f(t)\cos(\omega t)$, where $f(t) = \exp[-2\ln(2)(\frac{t}{\tau_d})^2]$ is the Gaussian envelope; the peak intensity of the laser pulse is chosen as 6×10^{14} W/cm^2. The frequency $\omega = 0.0569$ a.u. (800 nm in wavelength) and τ_d is the full-width at half-maximum (FWHM) of the laser field. $\tau_d = 3$ fs and $\tau_d = 5$ fs are considered respectively. The lasers' polarization directions are assumed to be parallel to the molecular axis in our calculations and the corresponding electric fields are shown in Fig. 2.

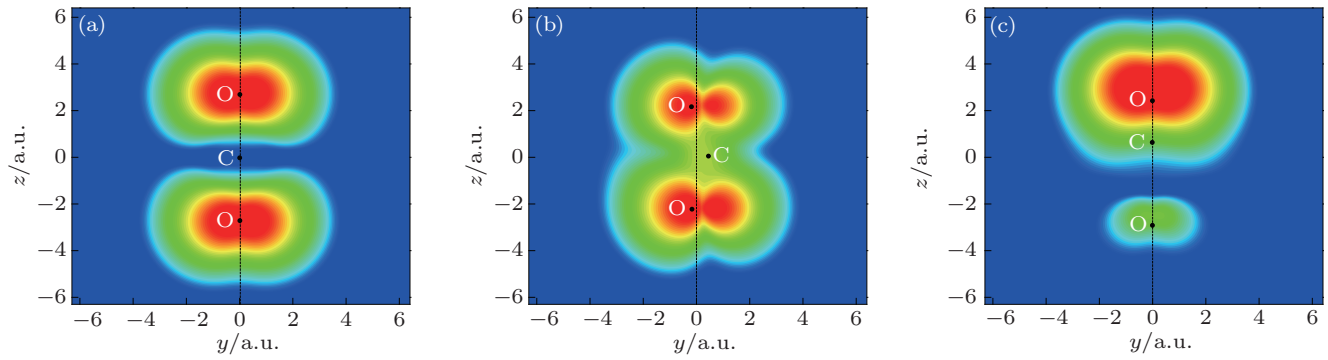


Fig. 1. (color online) The electron density of coordinate–space orbital $|\varphi(r)|^2$ of the HOMO of CO_2 molecule with (a) balance vibrational mode, (b) bending vibrational mode and (c) stretching vibrational mode.

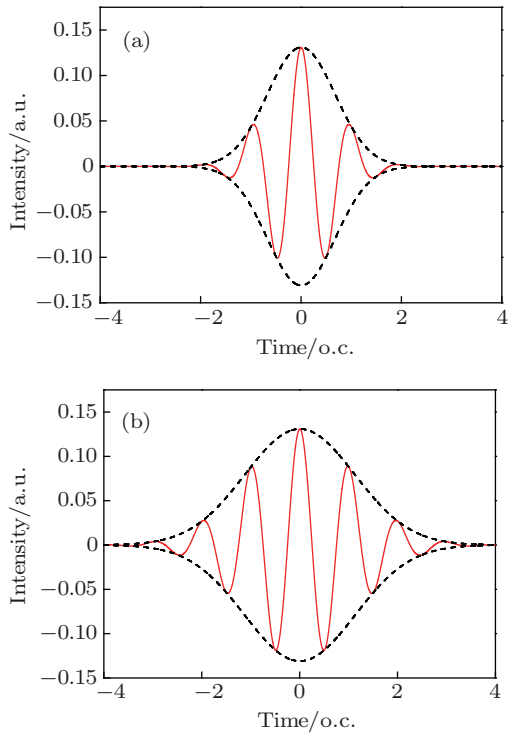


Fig. 2. (color online) The electric fields of the 800 nm laser pulse (red solid line) and corresponding pulse envelope (black dashed line) with (a) $\tau_d = 3$ fs, (b) $\tau_d = 5$ fs.

Figure 3 shows the HHG of the CO_2 molecule with different molecular vibrational modes for $\tau_d = 3$ fs and $\tau_d = 5$ fs. For $\tau_d = 3$ fs, figure 3(a) shows that the harmonic intensity of the CO_2 with the stretching vibrational mode is at least 3 orders of magnitude higher than that with the balance vibrational mode, and the intensity of the spectrum with the bending vibrational mode is a little stronger than that with the balance vibrational mode. These results indicate that the HHG spectrum is sensitive to molecular vibrational modes.

For $\tau_d = 5$ fs, figure 3(b) shows that the spectrums with three vibrational modes exhibit the similar tendency except more modulations compared with that for $\tau_d = 3$ fs.

Figure 4 shows the ionization yield of CO_2 molecule with different vibrational modes for the cases of $\tau_d = 3$ fs and $\tau_d = 5$ fs. It is clear to see that the ionization yield of CO_2 with the balance vibrational mode is the lowest, the ionization yield of CO_2 with the bending vibrational mode is a little enhanced and the ionization yield of CO_2 with the stretching vibrational mode is the largest, which results in the enhancement of HHG intensity with the stretching vibrational mode. We can find from Fig. 1 that the electron density distribution of the balance vibrational mode distributes around the two carbon nuclei and the electron density distribution of the stretching vibrational mode almost distributes around the carbon nucleus in the positive z direction. Electrons are attracted by two carbon nuclei in the balance vibrational mode, but in the stretching vibrational mode electrons feel the attractive forces mostly from one carbon nucleus, which may lead to the electrons being easy to ionize in the stretching vibrational mode.

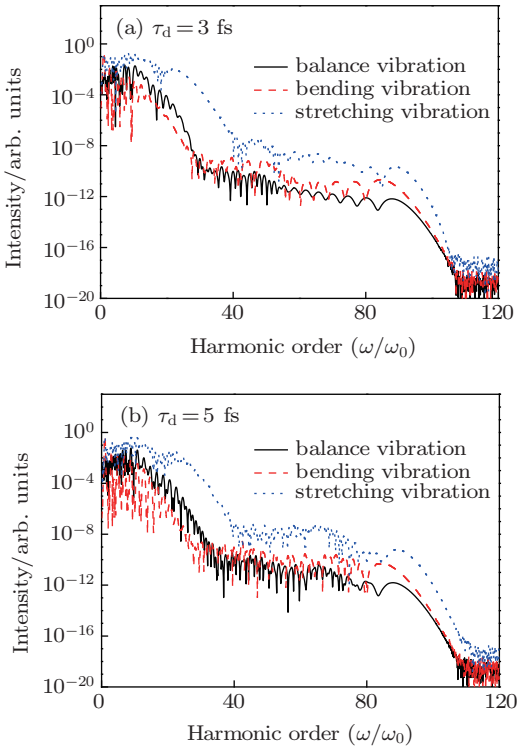


Fig. 3. (color online) The HHG of CO_2 with different vibrational modes in the intense laser field with the peak intensity of 6×10^{14} W/cm^2. (a) $\tau_d = 3$ fs, (b) $\tau_d = 5$ fs.

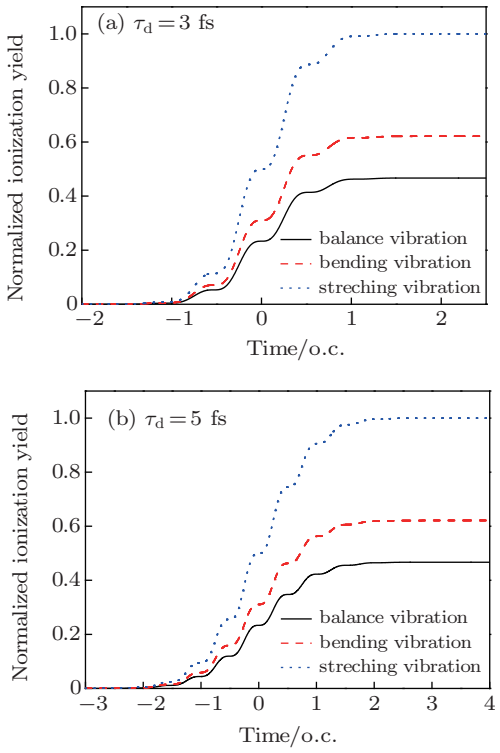


Fig. 4. (color online) Ionization yields of CO_2 molecule with different vibrational modes. (a) $\tau_d = 3$ fs, (b) $\tau_d = 5$ fs.

We investigate the time frequency distributions of harmonics from the 60th to 90th of CO_2 with different vibrational modes for the cases of $\tau_d = 3$ fs, which are shown

in Figs. 5(a)–5(c). It is clear to see that the intensity of the emission peaks with the stretching vibrational mode are the strongest, which is in accordance with the high harmonic generation and the corresponding ionization yields shown in Fig. 3(a) and Fig. 4(a).

Figures 5(d)–5(f) show the temporal profiles of the generated attosecond pulses from CO_2 by performing the inverse Fourier transforms of the spectrum with different vibrational modes. Figure 5(d) shows that, by properly filtering the harmonic spectrum from 54th to 82th with the balance vibrational mode, an isolated attosecond pulse with a duration of about 120 as is generated. An asec pulse train with two radiation pulses is generated with bending vibrational mode as depicted in figure 5(e) by superposing harmonics from the 61th to 83th order. Figure 5(f) shows that a strong and isolated asec pulse with a duration of about 112 as is obtained with the stretching vibrational mode by superposing the harmonics from the 57th to 83th order. Furthermore, the peak intensity of the asec pulse is gradually enhanced from Fig. 5(d) to Fig. 5(e), and the intensity of asec pulse with the stretching vibrational mode is about 3 orders of magnitude higher than that with the balance vibrational mode.

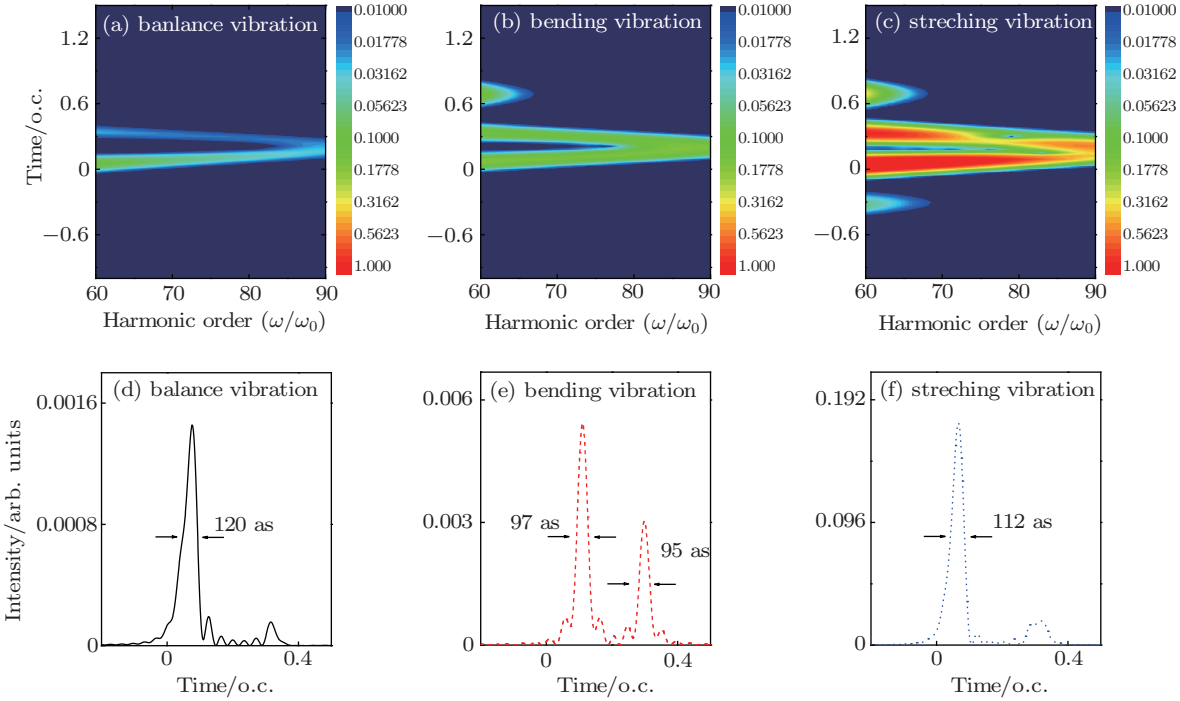


Fig. 5. (color online) (a)–(c) Time frequency distributions of harmonics from 60th to 90th and (d)–(f) the temporal profiles of generated attosecond pulses from CO_2 with different vibrational modes for the case of $\tau_d = 3$ fs.

4. Conclusions

We demonstrate the generation of high-order harmonic and attosecond pulse of CO_2 with different vibrational modes by the strong-field Lewenstein model. The results show that the high-order harmonic yield is sensitive to the molecular vibrational mode, and the efficiency of harmonic spectrum from CO_2 with the stretching vibrational mode is the strongest. The underlying physical mechanism of the HHG can be well explained by the corresponding ionization yields and the time-frequency analysis. When the CO_2 molecule with the stretching vibrational mode is exposed in the intense laser field with $\tau_d = 3$ fs, a strong isolated attosecond pulse with a duration of about 112 as is generated.

References

[1] Li P C, Laughlin C and Chu S I 2014 *Phys. Rev. A* **89** 023431
[2] Du H C, Wen Y Z, Wang X S and Hu B T 2014 *Chin. Phys. B* **23** 33202
[3] Zhang B, Yuan J and Zhao Z 2014 *Phys. Rev. A* **90** 035402
[4] Zhong H Y, Guo J, Zhang H D, Du H and Liu X S 2015 *Chin. Phys. B* **24** 73202
[5] Lu R F, He H X, Guo Y H and Han K L 2009 *J. Phys. B: At. Mol. Opt. Phys.* **42** 225601
[6] Zhang J, Ge X L, Wang T, Xu T T, Guo J and Liu X S 2015 *Phys. Rev. A* **92** 013418
[7] Lewenstein M, Balcou P, Ivanov M Y, L'Huillier A and Corkum P B 1994 *Phys. Rev. A* **49** 2117
[8] Corkum P B 1993 *Phys. Rev. Lett.* **71** 1993
[9] Schafer K J, Yang B, DiMauro L F and Kulander K C 1993 *Phys. Rev. Lett.* **70** 1599
[10] Maurer J, Dimitrovski D, Christensen L, Madsen L B and Stapelfeldt H 2012 *Phys. Rev. Lett.* **109** 123001
[11] Goulielmakis E, Loh Z H, Wirth A, *et al.* 2010 *Nature* **466** 739
[12] Zhang C P and Miao X Y 2015 *Chin. Phys. B* **24** 043302
[13] Pan Y, Zhao S F and Zhou X X 2013 *Phys. Rev. A* **87** 035805
[14] Cabasse A, Hazera C, Quintard L, Cormier E, Petit S and Constant E 2016 *J. Phys. B: At. Mol. Opt. Phys.* **49** 85601
[15] He L, Lan P, Zhang Q, Zhai C, Wang F, Shi W and Lu P 2015 *Phys. Rev. A* **92** 043403
[16] Śpiewanowski M D and Madsen L B 2014 *Phys. Rev. A* **89** 043407
[17] Ge X L, Wang T, Guo J and Liu X S 2014 *Phys. Rev. A* **89** 023424
[18] Bandrauk A D, Chelkowski S and Lu H 2009 *J. Phys. B: At. Mol. Opt. Phys.* **42** 75602
[19] Zhu X, Zhang Q, Hong W, Lan P and Lu P 2011 *Opt. Express* **19** 437

[20] Lai X and Faria C F de M 2013 *Phys. Rev. A* **88** 013406
[21] Petretti S, Saenz A, Castro A and Decleva P 2013 *Chem. Phys.* **414** 45
[22] Tchitchekova D S, Lu H, Chelkowski S and Bandrauk A D 2011 *J. Phys. B: At. Mol. Opt. Phys.* **44** 65601
[23] Qin M, Zhu X, Li Y, Zhang Q, Lan P and Lu P 2014 *Phys. Rev. A* **89** 013410
[24] Jin C, Le A T and Lin C D 2011 *Phys. Rev. A* **83** 053409
[25] Smirnova O, Mairesse Y, Patchkovskii S, Dudovich N, Villeneuve D, Corkum P and Ivanov M Y 2009 *Nature* **460** 972
[26] Chen Y J and Hu B 2009 *J. Chem. Phys.* **131** 244109
[27] Peters M, Nguyen-Dang T T, Cornaggia C, Saugout S, Charron E, Keller A and Atabek O 2011 *Phys. Rev. A* **83** 051403(R)
[28] Zhu X, Zhang Q, Hong W, Lu P and Xu Z 2011 *Opt. Express* **19** 13723
[29] Torres R, Kajumba N, Underwood J G, Robinson J S, Baker S, Tisch J W G, de Nalda R, Bryan W A, Velotta R, Altucci C, Turcu I C E and Marangos J P 2007 *Phys. Rev. Lett.* **98** 203007
[30] Le A T, Lucchese R R and Lin C D 2013 *Phys. Rev. A* **87** 063406
[31] Guo J, Zhong H, Yan B, Chen Y, Jiang Y, Wang T, Shao J, Zheng C and Liu X S 2016 *Phys. Rev. A* **93** 033806
[32] Wardlow A and Dundas D 2016 *Phys. Rev. A* **93** 023428
[33] Chang Z 2005 *Phys. Rev. A* **71** 023813
[34] Etches A and Madsen L B 2010 *J. Phys. B: At. Mol. Opt. Phys.* **43** 155602
[35] Guest M F, Bush I J, Van Dam H J J, Sherwood P, Thomas J M H, Van Lenthe J H, Havenith R W A and Kendrick J 2005 *Mol. Phys.* **103** 719